

Titania nano-coated quartz wool for the photocatalytic mineralisation of emerging organic contaminants

M. Saracino, L. Pretali, M. L. Capobianco, S. S. Emmi, M. L. Navacchia, F. Bezzi, C. Mingazzini, E. Burresti and A. Zanelli

ABSTRACT

Many emerging contaminants pass through conventional wastewater treatment plants, contaminating surface and drinking water. The implementation of advanced oxidation processes in existing plants for emerging contaminant remediation is one of the challenges for the enhancement of water quality in the industrialised countries. This paper reports on the production of a TiO₂ nano-layer on quartz wool in a relevant amount, its characterisation by X-ray diffraction and scanning electron microscopy, and its use as a photocatalyst under ultraviolet radiation for the simultaneous mineralisation of five emerging organic contaminants (benzophenone-3, benzophenone-4, carbamazepine, diclofenac, and triton X-100) dissolved in deionised water and tap water. This treatment was compared with direct ultraviolet photolysis and with photocatalytic degradation on commercial TiO₂ micropearls. The disappearance of every pollutant was measured by high performance liquid chromatography and mineralisation was assessed by the determination of total organic carbon. After 4 hours of treatment with the TiO₂ nano-coated quartz wool, the mineralisation exceeds 90% in deionised water and is about 70% in tap water. This catalyst was reused for seven cycles without significant efficiency loss.

Key words | advanced oxidation processes, emerging organic contaminants, photocatalysis, titanium dioxide

M. Saracino
L. Pretali
M. L. Capobianco
S. S. Emmi
M. L. Navacchia
A. Zanelli (corresponding author)
 Consiglio Nazionale delle Ricerche (CNR),
 Istituto per la Sintesi Organica e la Fotoreattività
 (ISOF),
 101, via P. Gobetti, Bologna I-40129,
 Italy
 E-mail: alberto.zanelli@isof.cnr.it

M. Saracino
 Dipartimento di Chimica Industriale 'T. Montanari',
 Università degli Studi di Bologna,
 6, Viale Risorgimento, Bologna I-40134,
 Italy

F. Bezzi
C. Mingazzini
 ENEA SSPT-PROMAS-TEMAF,
 Laboratory of Materials Technologies,
 186 via Ravegnana, Faenza I-48018,
 Italy

E. Burresti
 ENEA SSPT-PROMAS-MATAS,
 Brindisi Research Center,
 S.S. 7 Appia Km 706, Brindisi I-72100,
 Italy

INTRODUCTION

The last amendment of the Water Framework Directive 2000/60/EC introduces a 'watch list' of aquatic contaminants that contains seven pesticides, six pharmaceuticals, an antioxidant, and a personal care product with the aim of monitoring them and understanding if quality standard references should be imposed. In addition to the substances regulated by the European Directives, a new group of molecules, called emerging organic contaminants (EOCs), is becoming of concern. EOCs, defined as organic compounds that have no regulatory standard, include newly commercialised chemicals just introduced in the environment, or those already monitored but

whose presence and significance are not yet clear (Daughton 2004). Many pharmaceutical and personal care products, and residues of industrial activity are considered EOCs. Globally, EOC concentrations measured in the aquatic environment range from ng L⁻¹ to µg L⁻¹, and only the recent development of sensitive analytical techniques has enabled the detection of such low concentrations both in surface and drinking water. The poor knowledge of EOC middle- or long-term impacts on aquatic environments and some evidence of their endocrine-disrupting activity has stimulated several surveys on their occurrence in many countries (Balmer *et al.* 2005; Loos *et al.* 2010). In some effluents from pharmaceutical manufacturing factories, and in some influents to wastewater treatment plants (WWTPs), the maximum concentration of some pharmaceuticals has been found in the order of mg L⁻¹ [i.e. ciprofloxacin 31 mg L⁻¹ (Larsson 2014), venlafaxine 11.7 mg L⁻¹ and carbamazepine

This is an Open Access article distributed under the terms of the Creative Commons Attribution Licence (CC BY-NC-SA 4.0), which permits copying, adaptation and redistribution for non-commercial purposes, provided the contribution is distributed under the same licence as the original, and the original work is properly cited (<http://creativecommons.org/licenses/by-nc-sa/4.0/>).

doi: 10.2166/wst.2017.457

(CBZ) 0.84 mg L⁻¹ (Lester *et al.* 2013), and diclofenac (DCF) 0.2 mg L⁻¹ (Ratola *et al.* 2012)].

The WWTPs, originally not designed to handle EOCs, might be considered mainly responsible for their transfer to water bodies and consequent accumulation (Oulton *et al.* 2010). EOC removal can be accomplished only by using new technologies (Tuerk *et al.* 2010) such as the advanced oxidation processes (AOPs).

Ultraviolet (UV) radiation in the wavelength range 100–280 nm is widely used for wastewater disinfection and, in some cases, it may lead to the direct photolysis of photolabile compounds (Zuccato *et al.* 2010). The photochemical activity of UV radiation can be converted to an oxidative effect by coupling it with appropriate additives and photocatalysts (McCullagh *et al.* 2011). TiO₂ is known to be an effective water disinfection option, since it does not need the addition of chemicals which can react together to form toxic by-products as, for instance, in the case of chlorination. The absorption of UV light by TiO₂, in O₂-saturated H₂O, produces reactive species (mainly ·OH and ·O₂⁻) capable of degrading organic molecules in solution. Since its energy gap is 3.2 eV (Oppenlander 2003), TiO₂ is able to absorb solar radiation with wavelengths shorter than 385 nm. Thus, TiO₂-based photocatalytic processes seem not only sustainable and reliable solutions for a wide variety of water-remediation issues, but also economically advantageous. In fact, with respect to the last statements, even if artificial UV radiation is energy demanding, it is preferable to solar radiation for high water loads, because it can work 24 hours per day, it allows higher light power per unit volume of water (thus avoiding huge sunlight collecting surfaces), and it induces direct photolysis on a wider group of molecules.

The immobilisation of a photocatalyst on a UV-transparent solid is an advantage for practical use; some research has been devoted to TiO₂ immobilised on mineral fibres. Wang & Ku (2003) studied the coating of TiO₂ on a single quartz fibre for the abatement of benzene in air. Hue & Hang (2013) performed the degradation of 0.44 mg m⁻³ benzene in air with TiO₂-coated quartz cotton irradiated with 40 W UV light (400–315 nm), achieving the total decomposition of the contaminant in 4.5 hours, due to the transparency and the high surface area of the substrate. Horikoshi *et al.* (2002) achieved the partial photocatalytic mineralisation of a 0.1 mmol L⁻¹ nonylphenol polyoxytate aqueous solution after 6 hours of UV irradiation by using TiO₂ immobilised on fibreglass cloth by the sol-gel method.

The aim of the present study was to evaluate the possibility of producing large batches of photocatalyst nano-layers immobilised on a high-surface-area (per unit of

volume) solid substrate potentially transparent to UV light. The present work reports on the synthesis and the use of a TiO₂ nano-layer on quartz wool (TiO₂-qw) for the degradation of a mixture of five EOCs: benzophenone-3 (BP3), benzophenone-4 (BP4), CBZ, DCF and triton X-100 (TRX). Furthermore, this study was carried out both on deionised water (DW) and tap water (TW), in order to understand the degradation parameters of standardised samples before use on real WWTP effluents. The performance of TiO₂-qw was compared with that of commercial TiO₂ micropearls (TiO₂-mp), up to now considered the most efficient on the market (Kanakaraju *et al.* 2014a, 2014b), and with that of direct UV photolysis. The TiO₂-qw life cycle was also evaluated.

The five EOCs selected for the present study, besides being some of the most frequently detected pollutants, belong to categories showing different water affinities, and containing different chemical groups. Their structures and a short description of their use and occurrence in water bodies are reported in the Supporting Information (available with the online version of this paper).

METHODS

All chemicals were reagent grade and were used without any further purification. TiO₂ VP Aeroperl P25 20 from Evonik is the new brand of the well known Degussa P25. The average geometrical area has been estimated as 0.2 m² g⁻¹. Quartz wool (density 2.2–2.6 g cm⁻³) was supplied by Carlo Erba.

DW was produced by a MilliRO 15 water purification system (Millipore). TW was collected from municipal waterworks of Bologna, Italy, and the concentrations of the main metals and anions are listed in Table SI2 (available with the online version of this paper) with total organic carbon (TOC), light absorbance and conductivity.

TiO₂-qw was produced by the deposition of a TiO₂ thin film on quartz wool by the sol-gel technique. The sol was obtained by mixing titanium tetraisopropoxide, absolute ethanol, acetylacetone and 1 mol L⁻¹ HCl aqueous solution in 1:0.5:3:34 ratios. Acetylacetone was used as a complexant in order to avoid the precipitation of titanium byproducts, whereas HCl was added in order to introduce the required amount of water and to promote the polymeric sol synthesis by acidic catalysis.

Four specimens of the sol were dried under atmospheric conditions up to sol-gel transition and the solvent evaporation was completed under infrared lamp, then the solids were treated for 30 min at 350, 400, 450, and 500 °C, respectively.

The quartz wool (Figure S11, available with the online version of this paper) was soaked in the TiO₂ sol previously diluted in ethanol with a volume ratio of 1:5. This dilution ratio was chosen in order to avoid a thick deposition on the fibres, which would exhibit fragile behaviour and low adhesion. The solvent was then evaporated under atmospheric conditions for about 20 min and the densification was performed for 30 min at 450 °C (the temperature selected after X-ray diffraction (XRD) studies of the above-mentioned four specimens). The obtained samples were washed with water to remove the unbound TiO₂ and dried at 120 °C for 20 min. A loading of 35 mg of TiO₂ per gram of TiO₂-qw was determined by weight.

The scanning electron microscopy (SEM) observations were performed on TiO₂-qw with the scanning electron microscope Leo 438 VP, using both secondary electrons and backscattering electron detectors, in partial vacuum conditions, with and without sample metallisation. Absorbance was evaluated by Perkin-Elmer Lambda 9 spectrophotometer.

The light source was a Multilamp Rayonet provided with 16 lamps (Sylvania G8 W) with emission maximum centred at 254 nm and absorbed power 8 W (UV flux in the centre of the reactor was 25 mW cm⁻²) and an air blowing cooler. The experiments were carried out in a quartz tube (diameter 4 cm) equipped with a condenser, a thermometer, and a Teflon capillary pipeline to supply the air bubbles that provided the stirring and suspended the catalyst particles. The tube was filled with 0.25 L of the DW or TW solution containing C₀ = 5 mg L⁻¹ of each contaminant, that is the same order of magnitude of the highest concentration detected in effluents of pharmaceutical manufacturing (Ratola *et al.* 2012; Lester *et al.* 2013; Larsson 2014). Three samples of the solutions were treated as follows: (i) UV radiation and air; (ii) UV radiation, 25 mg TiO₂-mp and air; and (iii) UV radiation, 1 g TiO₂-qw and air. 5 mL samples were withdrawn at specific times and stored in the dark at 4 °C before the analysis. In the case of the TiO₂-mp suspension, the samples were centrifuged before the analysis.

The concentration of the contaminants was determined using a high performance liquid chromatograph (HPLC) Agilent 1260, equipped with a diode array detector and a luminescence detector. Sample injection volume was 40 µL and analytes were separated on a reverse phase Zorbax C8 column (4.6 × 150 mm, 5 µm). A linear gradient from 0.1% trifluoroacetic acid in water to 100% acetonitrile at 1.0 mL min⁻¹ flow rate was used. The detection was carried out at 285 nm for all the compounds, with the exception of TRX which was detected by using the in-line Varian Pro Star 363 fluorescence detector ($\lambda_{\text{ex}} = 229$ nm and $\lambda_{\text{em}} = 302$ nm).

TOC concentration was measured by means of a Hach-Lange DR5000 spectrophotometer and LCK-385 test-in-cuvette with limit of quantification (LOQ) 3 mg L⁻¹ and uncertainly 15%. The pH was measured by an Orion Research Expandable Ion analyzer EA940 equipped with a Hanna Instruments HI 1111 electrode. When possible pH was reported as the average value of several different solutions with its standard deviation (SD).

RESULTS AND DISCUSSION

TiO₂-qw studies

In the four powder specimens, the two main TiO₂ phases, anatase and rutile, were confirmed by XRD (Figure S12, available with the online version of this paper). Anatase, the phase with the most promising photocatalytic activity (Oppenlander 2003), appeared after treatment at 350 °C, but mainly in amorphous form. The rutile phase was detected at 500 °C together with anatase of the highest crystallinity compared to that observed after thermal treatment at lower temperatures. On the basis of the XRD results, a temperature of 450 °C was chosen for the densification of TiO₂ nano-coating on a relevant amount of quartz wool (about 50 g), in order to obtain anatase with the highest crystallinity together with the minimum content of the rutile phase.

The SEM characterisation of the TiO₂-qw was done on specimens with and without gold sputtering. In both cases, very good resolutions were obtained, but observations without sputtering and using the secondary electron partial vacuum detector were preferred, in order to avoid any possible interference from gold deposition. The backscattering electron detector was used to find the coating defects, exploiting its sensitivity to the mean atomic weight, which is lower for quartz than for titania. Some micrographs of the obtained coated quartz fibres before use are shown in Figure 1. The diameter of the fibres spans from 6 to 20 µm, consequently the TiO₂-qw geometric surface is estimated in the range 0.28–0.08 m² g⁻¹, which is comparable to that of TiO₂-mp. Because of the characteristics of the quartz substrate and because of the coating method (dipping in a precursor solution, gelling and drying), very variable coating thicknesses and also defects were observed. In particular, some fibres show crystallites grown perpendicularly to the fibre axis and, sometimes, mass accumulation appears near the fibre crossings. Finally, some collar-shaped defects appear, showing the presence of the coating and its

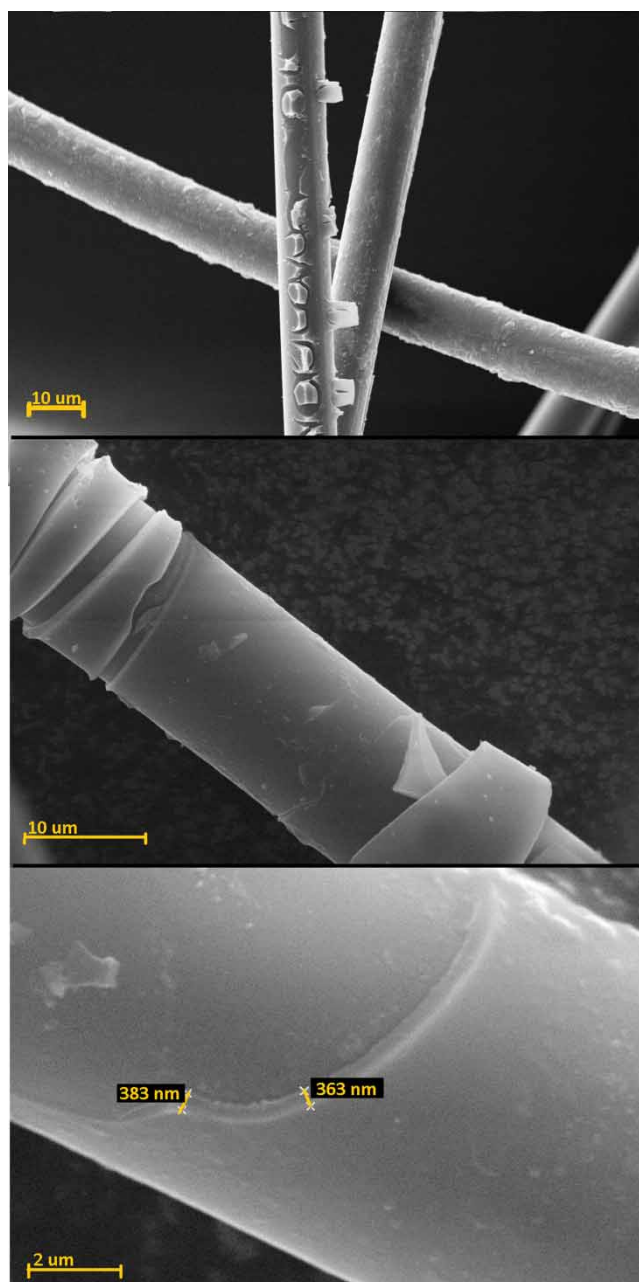


Figure 1 | SEM images of TiO₂-qw before use (secondary electron detector in partial vacuum conditions). Thickness data are reported on a sample without gold coverage.

occasional collapse along the fibre axis during the early deposition phase. In the region without defects, the thickness of the TiO₂ coating is about 400 nm.

Degradation of the EOCs

Figure 2 shows the percentage ratio of the residual concentration C_t and the initial concentration C_0 of the five EOCs

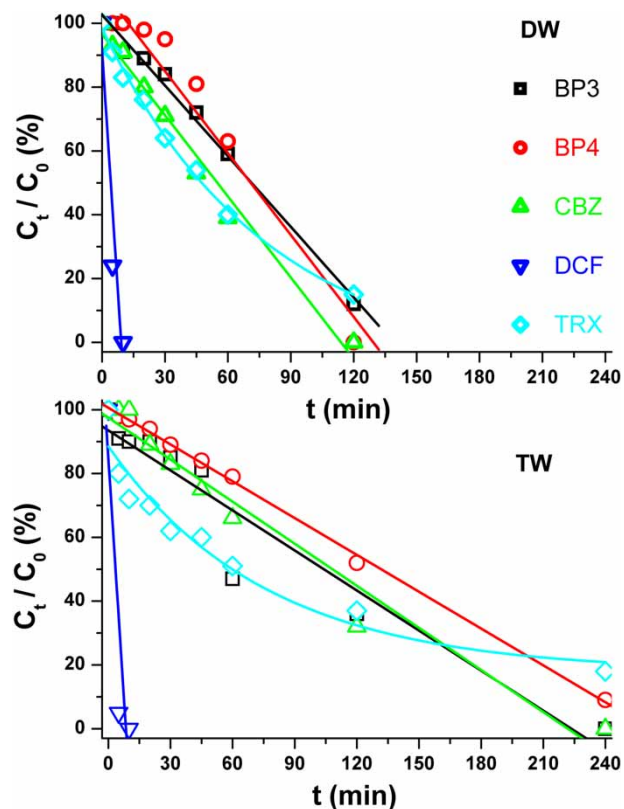


Figure 2 | Residual content of the five EOCs treated with UV light and air in DW and TW.

after UV irradiation and is considered the reference experiment for the following photocatalytic treatments. DCF, due to its photosensitivity, completely disappears after 5 min of irradiation both in DW and TW. The concentration of the other EOCs in DW show decreases of about one order of magnitude after 120 min, roughly following zero-order kinetics. All these five molecules, like many other EOCs, contain UV-sensitive aromatic systems whose excited species may start photochemical reactions involving dissolved O₂.

In TW: BP3, BP4, and CBZ need about 240 min to decrease their concentration by one order of magnitude, whereas TRX does not reach this goal. The slower degradation in TW is likely to be due to inorganic ions which inhibit the process by scavenging the active radicals.

During the UV treatment in DW, as well as during the photocatalytic ones described below, pH decreases from neutral values (average 7.8, SD 0.5) to a value ranging from 4.3 to 5.6, typical values of the carboxylic acid solutions. On the other hand, in TW the initial pH (average 7.9, SD 0.3) is similar to that in DW, but it increases to about 8.3–9.2 (after the treatment with TiO₂-qw in TW average pH was 8.3, SD 0.3) indicating that the scavenging of the active radicals opens alternative pathways to the formation of carboxylic acids.

The samples irradiated up to about 60 min show a yellowish coloration, and the corresponding HPLC analysis have a slightly increased baseline signal, indicating the presence of byproducts. However, their concentrations were too low to be detectable by our analytic procedure.

UV irradiation in the presence of 0.1 g L⁻¹ suspended TiO₂-mp in DW – that is reported as one of the best TiO₂ concentrations (Mendez-Arriaga et al. 2008) – if compared to UV radiation alone, does not enhance appreciably the disappearance rate of DCF and CBZ, but speeds up the degradation of BP3 and BP4, shifting the disappearance half-life from 72 min to 56 and 63 min, respectively; and that of TRX from 56 min to 46 min (Figure 3 DW). Also the use of TiO₂-mp in TW generally speeds up the disappearance rate of the contaminants, but it also seems to change the kinetics from zero-order to pseudo-first-order (Rizzo et al. 2009) or to a mechanism combining two consecutive steps with different kinetics (Figure 3 TW). The kinetics of Degussa P25 photocatalysis has been clearly explained elsewhere (Xiong & Hu 2012).

In a recent study (Kanakaraju et al. 2014a, 2014b), 30 mg L⁻¹ of DCF in distilled water were subjected to a

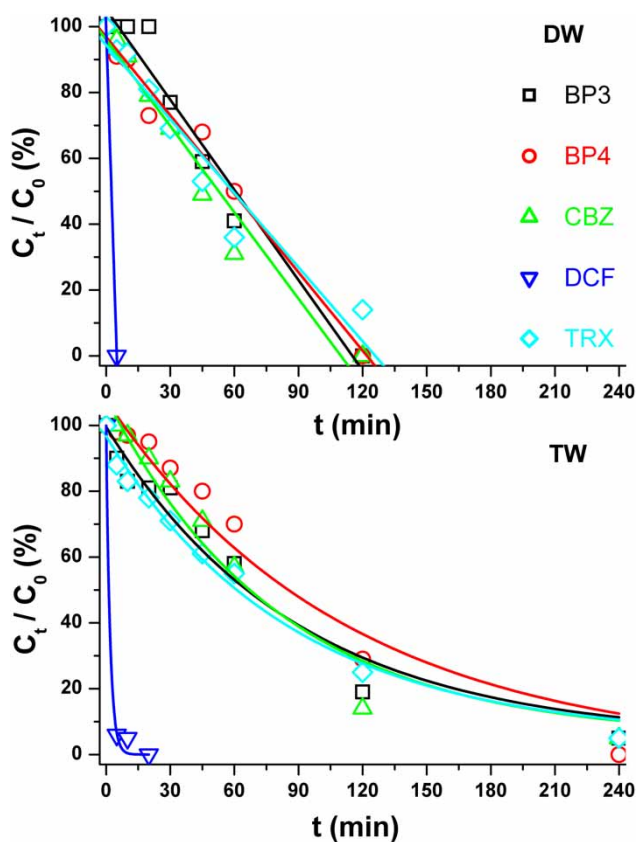


Figure 3 | Residual content of the five EOCs treated with TiO₂-mp, UV light and air in DW and TW.

Table 1 | Variation of the concentration of some inorganic ions before and after treatment with TiO₂-mp, UV light and air in TW

Parameter	Before treatment	After 240 min	Units
pH	7.6	9.0	–
CO ₃ ²⁻	0	3.6	mg L ⁻¹
HCO ₃ ⁻	226.5	49.9	mg L ⁻¹

UV photocatalytic treatment (TiO₂ Degussa P25 loading 0.1 g L⁻¹), achieving complete removal after 15 min, when sunlight photochemical degradation required up to 360 min of exposure. TOC was not evaluated but six photo-products were detected. Also in this study, DCF in TW showed higher pseudo-first-order rate constants, confirming matrix effect on the degradation rate. Similar confirmation comes from a study on a photocatalytic process (TiO₂ 0.02–0.5 g L⁻¹; light 400–315 nm, 250–400 W) where the removal efficiency of the 5 mg L⁻¹ CBZ alone declined by 30% when the matrix was changed from distilled water to a groundwater having pH 7.5 and conductivity 0.79 mS cm⁻¹ (Shirazi et al. 2013).

The inorganic components of TW before and after the treatment with TiO₂-mp under UV irradiation remain almost unaltered except for those reported in Table 1. On the other hand, the concentrations of carbonate and bicarbonate are in the same order of magnitude of EOC concentrations but are several orders of magnitude higher than that of halides (Table SI2). We observe the increase of pH and the decrease of HCO₃⁻ concentration that we explain with CO₂ evolution that consumes the H⁺ produced in the oxidation processes. On the other hand, the scavenging converts ·OH to OH⁻, increasing the alkalinity (Buxton et al. 1988; Grebel et al. 2010). Other authors report that CO₃²⁻ is also responsible for a slower absorption of EOCs on the TiO₂ surface (Guillard et al. 2005).

The use of 1.0 g TiO₂-qw per experiment, corresponding to an estimated maximum value of 0.14 g L⁻¹ of TiO₂, almost doubles the disappearance rate of the EOCs (Figure 4), both in DW and TW, with respect to the TiO₂-mp treatment (Figure 3). For example, the time for the 50% removal of TRX in DW shifts from 56 to 12 min, and in TW from 61 to 26 min.

Only the DCF degradation rate was not enhanced because direct photolysis largely remains faster than photocatalysis. The TiO₂-qw samples are in the shape of a wool ball with a diameter of 4 cm and an apparent density of about 30 mg cm⁻³. The TiO₂-qw absorption and scattering of the 254 nm light increased by about 10% per mg cm⁻³ of apparent density. With this geometry a fraction of the

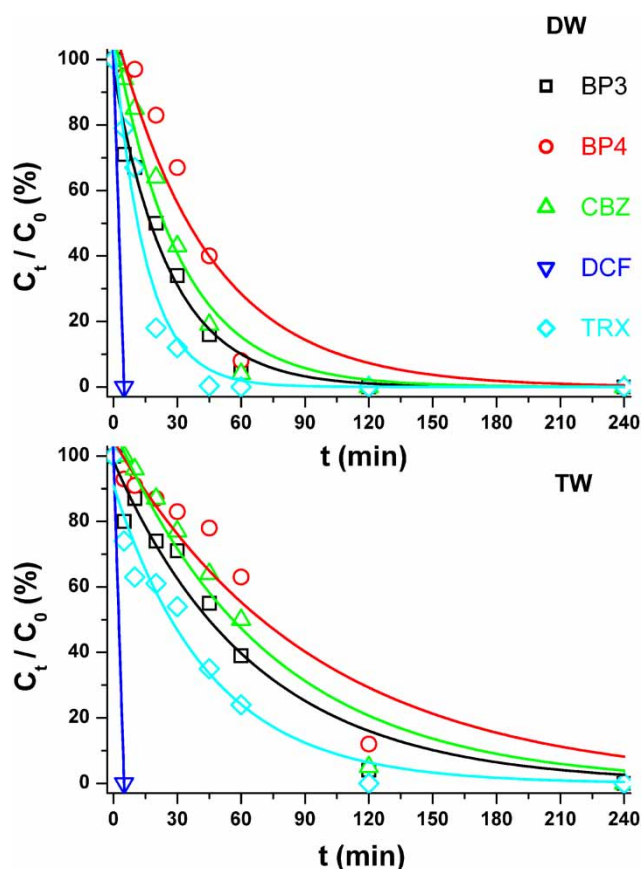


Figure 4 | Residual content of the five EOCs treated with TiO₂-qw, UV light and air in DW and TW.

TiO₂-qw does not receive light, however, better performances could be achieved by changing the reaction geometry or by reducing the apparent density of the catalyst substrate composite.

Mineralisation and catalyst life-cycle

Figure 5 compares the average residual content of the five EOCs after 120 min (initial EOC concentration $C_0 = 25 \text{ mg L}^{-1}$) and the residual TOC after 240 min (theoretical initial TOC $C_0 = 15.9 \text{ mg L}^{-1}$), in the two water matrices. The temperature during all six experiments increases in the same way from $24 \pm 2 \text{ }^\circ\text{C}$ to $53 \pm 2 \text{ }^\circ\text{C}$, making a homogeneous contribution to the degradation rates. In DW the three treatments, after 120 min, reduce the total EOC concentration by one order of magnitude or more, but in TW, only the AOP treatment with TiO₂-qw is able to reach this goal (Figure 5(a)). Also the opposite trends of pH in DW and TW suggests different degradation pathways depending on the matrices.

In the case of TW, the EOC mineralisation needs longer times than in DW (Figure 5(b)). Even if in DW the three mineralisation processes can be considered satisfactory after 240 min, in TW, UV mineralises only the 30% of the EOCs. However, photocatalysis significantly enhances the EOC mineralisation process, achieving the best performance with TiO₂-qw (residual TOC about 30%). The advantage in this case is that a larger photocatalytic area is exploited, compared with the same amount of TiO₂-mp. Furthermore, the use of a solid support facilitates the recovery and reuse of the catalyst itself.

Figure 6 shows the performance of TiO₂-qw in TW on TOC (dots) and EOC average concentration (squares) over repeated cycles of UV irradiation in the presence of air bubbling. After every 240 min long treatment, TiO₂-qw was recovered, washed three times in DW to remove residual salts and organic matter, dried at 120 °C for 18 hours and weighed. The weight loss after every cycle was less than 0.5%. The fitting to a constant residual content shows that the average EOC residual after 120 min (12%) stays within the confidence band (confidence level 95%), but TOC residual after 240 min (45%) at the eighth cycle exceeds the confidence band. The energy spent to degrade a gram of EOCs, evaluated after Bolton *et al.* (2001), was $47 \pm 2 \text{ kWh g}^{-1}$, and the energy spent to mineralise a gram of

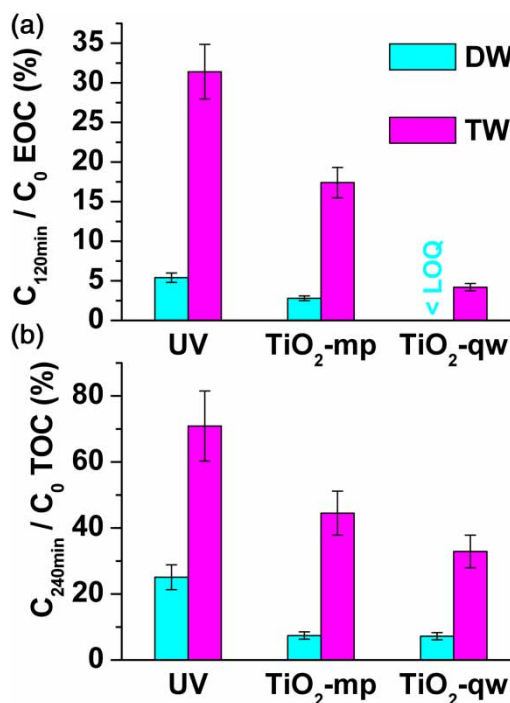


Figure 5 | Residual EOC content after 120 min (a) and residual TOC content after 240 min (b) of the three treatments.

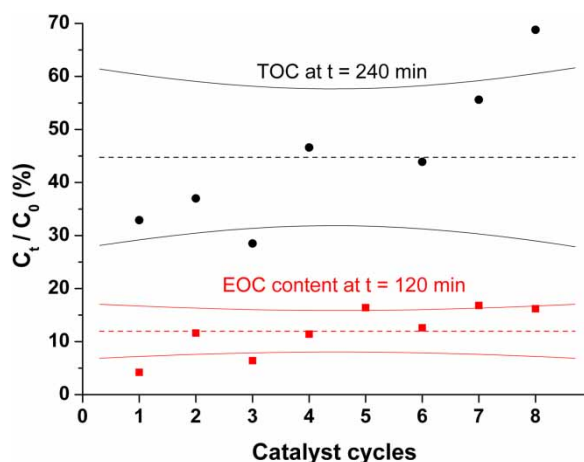


Figure 6 | Residual EOC content after 120 min and residual TOC after 240 min of repeated treatments with TiO₂-qw, UV light and air in TW. The dashed lines show the linear fitting to constant residues and the curves the related confidence bands.

EOCs was $230 \pm 40 \text{ kWh g}^{-1}$. These results are evaluated on the basis of the nominal electric absorption of the UV lamps but the high power of the lamps, 128 W, was chosen in order to exceed the absorption of both the catalysts and compare them at their maximum activity. Furthermore, the geometry of the stationary photoreactor does not ensure the complete absorption of the emitted radiation. Studies with a flow reactor with optimised geometry are in progress and the use of LED UV sources is under evaluation (Xiong & Hu 2012).

After working for eight cycles, the TiO₂-qw was analysed by SEM once again and the images are shown in Figure 7. A comparison of these images with those of Figure 2 demonstrates that the coating morphology of the catalyst was essentially unchanged after eight cycles even if a loss of TiO₂ appears in the defects and thicker points.

CONCLUSIONS

The sol-gel method is suitable for producing a nanometric layer of TiO₂ on an amount of quartz wool with a satisfactory adhesion and homogeneity, which has never been reported before.

The simple treatment with UV light and air, already used as a sanitising post-treatment in WWTPs, if correctly powered and coupled with air can significantly decrease the concentration of the five molecules selected as representative of the EOC main categories, but it does not mineralise the byproducts in TW. Direct UV absorption generates excited states of EOCs which degrades them to photostable organic compounds, but photocatalysis generates radicals

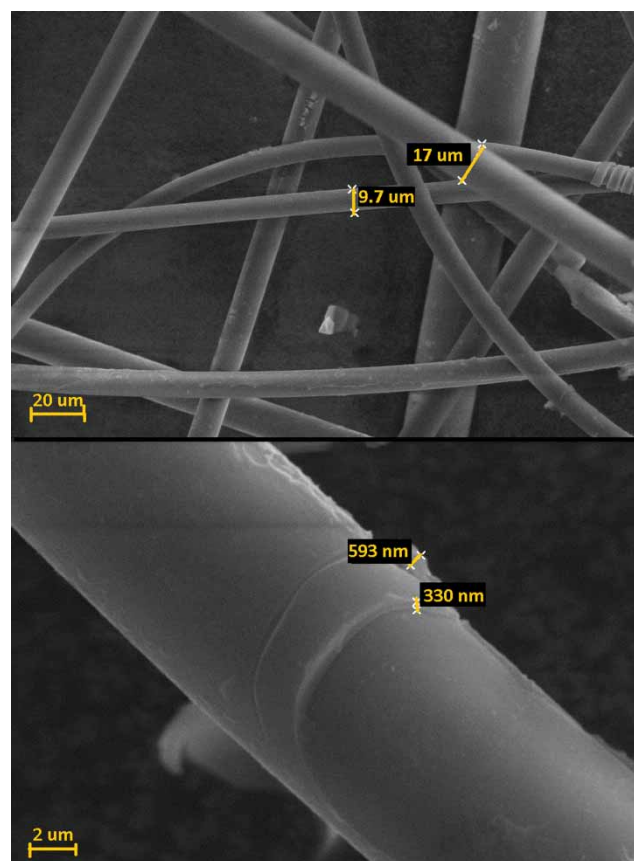


Figure 7 | SEM images of TiO₂-qw after eight treatments in TW (secondary electron detector in partial vacuum conditions).

from water which react both with EOCs and their photostable byproducts leading to the mineralisation. In fact, it can be envisaged that an expected inhibition of the process by TW inorganic ions affects the UV radicals more strongly than the photocatalytic ones.

TiO₂-qw leads to better performances with respect to a commercial TiO₂-mp suspension of similar mass of catalytic materials, because it allows a wider distribution of the photoactive material on the substrate surface. After 4 hours of UV irradiation on pristine TiO₂-qw, the mineralisation of the five selected EOCs exceeds 90% in DW and is about 70% in TW. Furthermore, TiO₂-qw has the advantage of being easily recovered and reused seven times without a relevant efficiency loss. Repeated treatments with TiO₂-qw in TW achieves an EOC degradation of about one order of magnitude and an average mineralisation of about 55% over seven consecutive cycles, making it a promising technology to abate those EOCs shown to be refractory to conventional wastewater treatments.

REFERENCES

- Balmer, M. E., Buser, H. R., Muller, M. D. & Poiger, T. 2005 Occurrence of some organic UV filters in wastewater, in surface waters, and in fish from Swiss lakes. *Environ. Sci. Technol.* **39** (4), 953–962. DOI: 10.1021/es040055r.
- Bolton, J. R., Bircher, K. G., Tumas, W. & Tolman, C. A. 2001 Figures-of-merit for the technical development and application of advanced oxidation technologies for both electric- and solar-driven systems. *Pure Appl. Chem.* **73** (4), 627–637. DOI: 10.1351/pac200173040627.
- Buxton, G. V., Greenstock, C. L., Helman, W. P. & Ross, A. B. 1988 Critical-review of rate constants for reactions of hydrated electrons, hydrogen-atoms and hydroxyl radicals ($\cdot\text{OH}/\text{O}^-$) in aqueous-solution. *J. Phys. Chem. Ref. Data* **17** (2) 513–886. DOI: 10.1063/1.555805.
- Daughton, C. G. 2004 Non-regulated water contaminants: emerging research. *Environ. Impact Assess. Rev.* **24** (7–8), 711–732. DOI: 10.1016/j.eiar.2004.06.003.
- Grebel, J. E., Pignatello, J. J. & Mitch, W. A. 2010 Effect of halide ions and carbonates on organic contaminant degradation by hydroxyl radical-based advanced oxidation processes in saline waters. *Environ. Sci. Technol.* **44** (17), 822–6828. DOI: 10.1021/es1010225.
- Guillard, C., Puzenat, E., Lachheb, H., Houas, A. & Herrmann, J. M. 2005 Why inorganic salts decrease the TiO₂ photocatalytic efficiency. *Int. J. Photoenergy* **7** (1), 1–9. DOI: 10.1155/s1110662x05000012.
- Horikoshi, S., Watanabe, N., Onishi, H., Hidaka, H. & Serpone, N. 2002 Photodecomposition of a nonylphenol polyethoxylate surfactant in a cylindrical photoreactor with TiO₂ immobilized fiberglass cloth. *Appl. Catal. B* **37** (2), 117–129. DOI: 10.1016/s0926-3373(01)00330-7.
- Hue, N. T. & Hang, D. T. T. 2013 Photocatalytic decomposition of benzene by UV illumination with the presence of nano-TiO₂. *Int. J. Nanotechnol.* **10** (3–4), 214–221. DOI: 10.1504/ijnt.2013.053134.
- Kanakaraju, D., Glass, B. D. & Oelgemoeller, M. 2014a Titanium dioxide photocatalysis for pharmaceutical wastewater treatment. *Environ. Chem. Lett.* **12** (1), 27–47. DOI: 10.1007/s10311-013-0428-0.
- Kanakaraju, D., Motti, C. A., Glass, B. D. & Oelgemoeller, M. 2014b Photolysis and TiO₂-catalysed degradation of diclofenac in surface and drinking water using circulating batch photoreactors. *Environ. Chem.* **11** (1), 51–62. DOI: 10.1071/en13098.
- Larsson, D. G. J. 2014 Pollution from drug manufacturing: review and perspectives. *Philos. Trans. R. Soc. B-Biol. Sci.* **369** (1656). DOI: 10.1098/rstb.2013.0571.
- Lester, Y., Mamane, H., Zucker, I. & Avisar, D. 2013 Treating wastewater from a pharmaceutical formulation facility by biological process and ozone. *Water Res.* **47** (13), 4349–4356. DOI: 10.1016/j.watres.2013.04.059.
- Loos, R., Locoro, G., Comero, S., Contini, S., Schwesig, D., Werres, F., Balsaa, P., Gans, O., Weiss, S., Blaha, L., Bolchi, M. & Gawlik, B. M. 2010 Pan-European survey on the occurrence of selected polar organic persistent pollutants in ground water. *Water Res.* **44** (14), 4115–4126. DOI: 10.1016/j.watres.2010.05.032.
- McCullagh, C., Skillen, N., Adams, M. & Robertson, P. K. J. 2011 Photocatalytic reactors for environmental remediation: a review. *J. Chem. Technol. Biotechnol.* **86** (8), 1002–1017. DOI: 10.1002/jctb.2650.
- Mendez-Arriaga, F., Esplugas, S. & Gimenez, J. 2008 Photocatalytic degradation of non-steroidal anti-inflammatory drugs with TiO₂ and simulated solar irradiation. *Water Res.* **42** (3), 585–594. DOI: 10.1016/j.watres.2007.08.002.
- Oppenlander, T. 2003 *Photochemical Purification of Water and Air*. Wiley-VCH Verlag, Weinheim, Germany, pp. 159–290.
- Oulton, R. L., Kohn, T. & Cwiertny, D. M. 2010 Pharmaceuticals and personal care products in effluent matrices: a survey of transformation and removal during wastewater treatment and implications for wastewater management. *J. Environ. Monitoring* **12** (11), 1956–1978. DOI: 10.1039/c0em00068.
- Ratola, N., Cincinelli, A., Alves, A. & Katsoyiannis, A. 2012 Occurrence of organic microcontaminants in the wastewater treatment process. A mini review. *J. Hazardous Mater.* **239**, 1–13. DOI: 10.1016/j.jhazmat.2012.05.040.
- Rizzo, L., Meric, S., Guida, M., Kassinos, D. & Belgiorno, V. 2009 Heterogenous photocatalytic degradation kinetics and detoxification of an urban wastewater treatment plant effluent contaminated with pharmaceuticals. *Water Res.* **43** (16), 4070–4078. DOI: 10.1016/j.watres.2009.06.046.
- Shirazi, E., Torabian, A. & Nabi-Bidhendi, G. 2013 Carbamazepine removal from groundwater: effectiveness of the TiO₂/UV, nanoparticulate zero-valent iron, and Fenton (NZVI/H₂O₂) processes. *Clean – Soil Air Water* **41** (11), 1062–1072. DOI: 10.1002/clen.201200222.
- Tuerk, J., Sayder, B., Boergers, A., Vitz, H., Kiffneyer, T. K. & Kabashi, S. 2010 Efficiency, costs and benefits of AOPS for removal of pharmaceuticals from the water cycle. *Water Sci. Technol.* **44** (11), 1167–1219. DOI: 10.2166/wst.2010.004.
- Wang, W. & Ku, Y. 2003 Photocatalytic degradation of gaseous benzene in air streams by using an optical fiber photoreactor. *J. Photochem. Photobiol. A* **159** (1), 47–59. DOI: 10.1016/s1010-6030(03)00111-4.
- Xiong, P. & Hu, J. 2012 Degradation of Acetaminophen by UVA/LED/TiO₂ process. *Separat. Purificat. Technol.* **91** (SI), 89–95. DOI: 10.1016/j.seppur.2011.11.012.
- Zuccato, E., Castiglioni, S., Bagnati, R., Melis, M. & Fanelli, R. 2010 Source, occurrence and fate of antibiotics in the Italian aquatic environment. *J. Hazardous Mater.* **179** (1–3), 1042–1048. DOI: 10.1016/j.jhazmat.2010.03.110.

First received 20 December 2016; accepted in revised form 1 August 2017. Available online 2 November 2017